Available online at www.sciencedirect.com
ScienceDirect
International Journal of Heat and Fluid Flow 29 (2008) 377–386
International Journal of HEAT AND FLUID FLOW
www.elsevier.com/locate/ijhff

Effect of hole imperfection on adiabatic film cooling effectiveness

M.B. Jovanović *, H.C. de Lange, A.A. van Steenhoven

Technische Universiteit Eindhoven, Department of Mechanical Engineering, Section Energy Technology, P.O. Box 513, 5600 MB Eindhoven, The Netherlands

Received 7 February 2006; received in revised form 23 October 2007; accepted 5 November 2007
Available online 29 January 2008

Abstract

The influence of a discrete imperfection on film cooling is studied by means of thermochromic liquid crystals measurements of the adiabatic film cooling effectiveness. As a benchmark, the effect of a jet ejected through a perfect hole is used. The film cooling effectiveness achieved with an imperfect hole is compared to the benchmark. A half torus plays the role of the discrete imperfection. The influence of the presence of the imperfection, its position and the turbulence intensity of the free stream are analyzed. The measurement data are depicted as two-dimensional plots but also as integral values. It is found that the imperfection, placed one diameter from the hole leading edge, deteriorates the effectiveness at moderate velocity ratios. Under the same conditions, the same imperfection fixed at the hole exit improves the effectiveness. At the velocity ratio of 1.50, the exit imperfection improves the integral effectiveness relatively for more than two times. The turbulence intensity and imperfections placed deeper in the hole do not have a significant influence.

Keywords: Jet in cross-flow; LCT; Film cooling; Imperfection; Effectiveness

1. Introduction

Gas turbines are used for aircraft propulsion, in land-based power generation and in industrial applications. The thermal efficiency and power output of a gas turbine rise with increasing turbine inlet temperature. In modern gas turbines, inlet temperature can reach 2000 K which exceeds the melting point of the blade and vane materials. Therefore, gas turbine elements must be cooled. One of a few methods used to cool gas turbine elements is film cooling. Cooling air is taken from the compressor stage and inserted into the boundary layer on a blade and/or vane surface with the aim to protect it from the hot gases, which come out of the combustion chamber. The cooling air is injected through holes into a blade boundary layer. These holes can be produced by means of a number of drilling techniques. One of these methods is laser drilling, which is a fast but also crude process. This can lead to the production of an irregular hole. Imperfections inside the film cooling hole are often discrete with a shape of a melt ejection. The imperfection can be relatively big and reach 25% of a hole diameter (see Allmen and Blatter, 1995). In this research we study how a discrete hole imperfection influences film cooling, when the film cooling process is simplified to a single jet in a cross-flow over a flat plate.

One of the first detailed investigation of a transverse jet in cross flow was reported by Bergeles et al. (1976). They found that the film cooling effectiveness strongly depends on the velocity ratio. The non-uniform velocity at the hole exit was detected with the peak near the hole trailing edge. An investigation on inner hole geometry can be found in Hale et al. (2000). They investigated the influence of a plenum on film cooling and found that the plenum geometry has an effect on the film cooling effectiveness, which depends on the injection hole length and streamwise hole angle. The effect of the hole length in the film cooling process was demonstrated in the study of Lutum and Johnson (1998). They reported that the length to diameter ratio larger than 7, has a small effect on the film cooling effectiveness. However, for shorter holes a decline of the hole length to diameter ratio decreases the film cooling effectiveness and the lowest value is detected for the shortest hole.

* Corresponding author. Fax: +31 40 243 3445.
E-mail addresses: m.jovanovic@tue.nl (M.B. Jovanović), h.c.d.lange@tue.nl (H.C. de Lange).

0142-727X/$ - see front matter © 2007 Elsevier Inc. All rights reserved.
doi:10.1016/j.ijheatfluidflow.2007.11.008

Cho et al. (1998) examined the hole orientation and its influence on film cooling. They showed that the holes with lateral injection angle produce better cooling. In Yuen and Martinez-Botas (2003) the adiabatic effectiveness was measured by means of liquid crystals. They investigated the influence of the blowing ratio and streamwise angle on the effectiveness. A hole inclination of 30° produces a higher effectiveness in comparison to the streamwise angle of 60° or 90°. They also reported that the region, with the effectiveness larger than 0.2, is not found beyond 13 diameters downstream from the hole. The hole outlet geometry affects film cooling strongly, e.g. Goldstein and Eckert (1974) conducted the experiments on shaped holes and found that, for blowing ratios above 0.5, the shaped hole produces much better effectiveness. Haven and Kurosaka (1997) examined the impact of the hole geometry on the development of flow structures. They showed that the hole geometry has an influence on the development of flow structures. By manipulating the hole geometry, the lift-off of the jet as well as the cross-flow entrainment can be regulated. A number of flow structures have been identified in the interaction region of the jet and cross-flow. The occurrence of these structures depends on local details of the geometry and flow conditions. Rutledge et al. (2005) investigated the influence of surface roughness on the heat transfer. Upstream roughness enlarges the boundary layer thickness by a factor of three. Therefore, the mixing is increased and the adiabatic effectiveness drops. The heat transfer coefficient is two times larger than on the smooth blade. Mayhew et al. (2003) measured the adiabatic film cooling effectiveness by means of liquid crystal thermography. They reported that free stream turbulence affects the cooling but it is not so significant and this influence can be neglected on higher blowing ratios. Many other parameters influence film cooling, too. Most of them have been studied on the ideal geometry. Jovanović et al. (2006) analyzed the effect of a discrete imperfection inside the short perpendicular hole. A windward vortex is detected in the imperfect case, while it is absent in the perfect case. This vortex reduces the film cooling effectiveness. The influence of the hole imperfection, located inside an inclined hole, on the flow field is reported in Jovanović et al. (2005). They found that the imperfection amplifies lee and windward vortices and leads to a bursting mechanism. The burst is detected in the case with the hole imperfection and it is absent in the perfect case.

The flow field for film cooling is characterized by 'weak' jets, which are ejected into the cross-flow boundary layer through inclined holes. In the interaction regions a number of coherent vortex structures have been recognized as depicted in Fig. 1. Haven and Kurosaka (1997) investigated experimentally the counter rotating vortex pair (CVP) and anti-CVP on varying hole shapes. They postulated that CVP originates at the side rims of the hole and they named it as steady kidney vortices. They have also discovered a double-decked structure. Two unsteady vortices roll above steady kidney vortices. According to the sign of their rotation these vortices can be unsteady kidney or unsteady anti-kidney vortices. They depict a heuristic model, capable to explain the flow field. Lim et al. (2001) investigated coherent structures of the jet in a cross-flow experimentally. They concluded that the cylindrical vortex sheet emerged from the hole underwent three distinct folding processes. One process leads to a formation of CVP and the other two form windward and lee vortices. These three vortical structures are independent. New et al. (2003) have formulated the folding process in details. Their paper mentions multiple scenarios of vortical rolls. The type and way of roll depend on the aspect ratio (hole shape) and mass-blowing ratio. The jet ejected through a short hole has been studied by Peterson and Plesniak (2004). A special attention has been put on the plenum orientation and its influence on the flow field. They investigated the jet cross-flow velocity field by means of PIV. The aforementioned structures have been visualized and quantified. Two steady vortices have been detected downstream of the hole. They have been named downstream spiral separation nodes, according to the flow topology. Guo et al. (2006) carried out a large-eddy simulation of the jet in cross-flow recently. The numerics has been able to detect large vortical structures reported in previous experimental works. In Jovanović (2007) results of PIV and LIF measurements are presented, which also proof that the flow field is dominated by four large vortical structures. These measurements revealed that the largest vortical structure is a counter rotating vortex pair, which finds its origin at the side-walls of the hole. This structure is capable of disposing main stream fluid into the wake region.

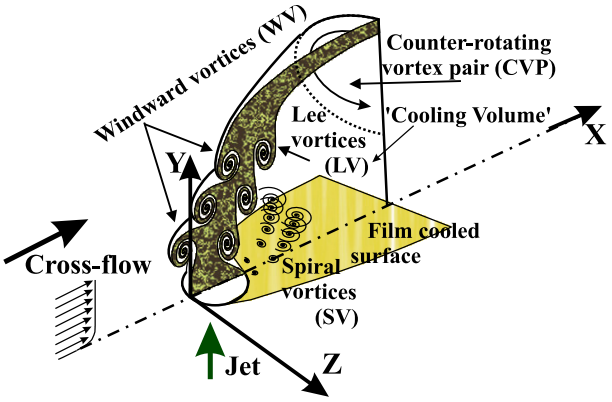

Fig. 1. Sketch of vortical structures generated by the jet cross-flow interaction according to Jovanović (2007).

Therefore, the object of this work is to investigate the influence of the imperfection, which is fixed inside the hole, on the adiabatic film cooling effectiveness. To this end experiments have been conducted at different velocity ratios with diverse imperfections. The position of a discrete imperfection is varied. Experiments have been conducted on multiple imperfections at two free stream turbulent intensities. The film cooling effectiveness was measured by means of liquid crystals thermography. The experimental set-up, measurement technique and uncertainties will be

described in Section 2. The results are presented as two-dimensional plots and integral values. The measurements conducted with an imperfect hole are compared to the benchmark (perfect hole). The answer to the question: 'How does the discrete hole imperfection change the adiabatic film cooling effectiveness?', will be addressed in Section 3. Negative as well as positive effects of imperfections will be shown and, where possible, connected to changes in the flow structures at the hole outlet.

2. Experimental apparatus and procedure

2.1. Experimental set-up

The experiments were conducted in a water channel at the Technische Universiteit Eindhoven (Eindhoven University of Technology) (for details see Jovanović et al., 2005). A plexiglas flat plate (2400 × 565 mm) is placed in the test section. The jet is ejected through the inclined smooth pipe into the cross-flow boundary layer. The leading edge of the jet hole is located 1625 mm from the plate leading edge (see Fig. 2a). The jet set-up is independent of the water channel and consists of a tank, pump, plenum and pipe. In our experiments the jet temperature is around 26 °C and the mainstream temperature is 20 °C. To simulate the process inside the turbine blade and to eliminate the influence of the pump, the plenum is fed symmetrically from the sides. At the inlet of the pipe the flow-straightener supported with a fine mesh is built-in to ensure homogeneous flow. The diameter of the pipe is $D = 57$ mm and the inclination angle is 37°. The length of the pipe L is equal to $10D$. Influence of different imperfections on the jet cross-flow interaction has been investigated and the blowing ratio has been

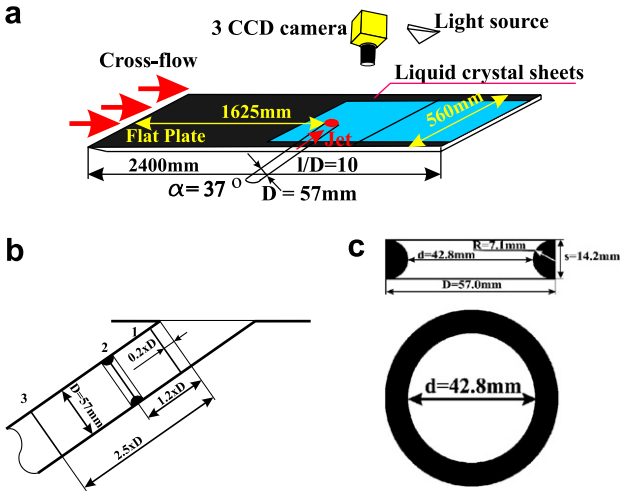

Fig. 2. Measurement set-up. (a) The set-up and its configuration for the LCT measurements in the water channel, (b) positions inside the hole on which the imperfection can be placed. The half-torus placed at the exit of the hole is called here inner-torus 1. Inner-torus 2 is at the second position and inner-torus 3 at the last one, (c) the top and cross-section view of the torus.

varied. It is well known that the jet cross-flow interaction is characterized mostly by means of the blowing ratio $\mathrm{BR} = \frac{\rho_{\mathrm{jet}}\overline{V}_{\mathrm{jet}}}{\rho_\infty V_\infty}$ and momentum ratio $\mathrm{MR} = \frac{\rho_{\mathrm{jet}}\overline{V}^2_{\mathrm{jet}}}{\rho_\infty V^2_\infty}$, where ρ_{jet} and ρ_∞ are the jet and cross-flow densities, $\overline{V}_{\mathrm{jet}}$ and V_∞ are the averaged velocity of the jet and the free stream velocity of the cross-flow, respectively. The cross-flow velocity is fixed at 0.2 m/s and it is constant in all experiments. This leads to an approaching boundary layer displacement thickness of about 5 mm with a Reynolds-number of about 1000.

Since the density is constant and the same fluid was used for the jet and cross-flow, the blowing ratio is equivalent to the velocity ratio $\mathrm{VR} = \frac{\overline{V}_{\mathrm{jet}}}{V_\infty} = \mathrm{BR} = \sqrt{\mathrm{MR}}$. The averaged jet velocity was calculated as the ratio of the jet volume flow and the pipe cross-section $\overline{V}_{\mathrm{jet}} = \frac{4\dot{Q}}{D^2\pi}$. Therefore, we will use only the velocity ratio to describe the jet flow. In our experiments VR will be varied between 0.15 and 1.5. This means that the Reynolds-number of the jet flow varies between 1700 and 17000.

The Reynolds-numbers of both the boundary layer and the jet flow are chose to match the conditions for film cooling of gas turbine blades. At low velocity the Reynolds number of the injected flow is small, therefore, it may be expected that the details of this scaling are important. On the other hand, the effect of the Reynolds-number of the approaching boundary layer will probably be minor, since the boundary layer thickness is very small in comparison to the hole diameter.

The experiments have been conducted with a smooth hole and hole which contains a discrete imperfection (see Fig. 2b). A case in which the jet is injected through the smooth pipe without any obstruction is called here the 'perfect case'. Experiments conducted with an imperfection inside the pipe are named as 'inner-torus' experiments. The discrete imperfection produced during the production process is simulated with a half-torus. The half-torus is a body defined by the intersection of the cylinder and the torus of the same radius. The size of the torus is equal to $D/8$, which leads to a hole-surface blockage of about 44%. In the experiments the position of the half-torus is changed. The imperfection has been placed on three different positions inside the hole (see Fig. 2b). The first position (IT1) is at the exit of the hole, in that case the torus central line was located $0.2D$ from the leading edge of the hole. The second position (IT2) is further inside, located at $1.2D$ from the leading edge of the hole. The deepest investigated imperfection (IT3) is placed $2.5D$ from the hole leading edge. To study the dominance of the imperfection and the effect of the multiple hole imperfections the three similar imperfections are simultaneously fixed inside the hole. This case is denoted as 'triple' imperfection. The turbulence intensity of the free stream is around 1%. To examine the influence of the turbulence intensity on the film cooling effectiveness a static grid is mounted at the entrance of the test section. The mesh size of the grid is 40 mm and

the rod diameter is 8 mm. The turbulence intensity, measured 620 mm from the grid is 7%.

2.2. Measurement techniques

Liquid crystal thermography has been used to measure temperature on the plate wall. To undertake these measurements two coated polyester sheets of thermochromic liquid crystals (TLCs) are fixed on the plate wall. The TLC sheets have been produced by Hallcrest (R20C5W). The red colour should start at 20° and the bandwidth is 5 °C. The measurements are conducted using wide band technique. The temperature in the channel has been measured by means of a mercury thermometer with an accuracy of 0.05 °C. The temperature in the channel is measured just before the beginning of an experiment. The jet temperature is adjusted and measured with the same thermometer to eliminate the bias. Images of the TLC sheets were taken with an analog three CCD video camera (JVC KY-F30). The camera is placed above the channel to look perpendicularly at the sheets. A light source is located at the side of the channel. To reduce reflection from the channel wall, the sheets are illuminated at an angle of approximately 45°. Each measurement is conducted during 60 s and stored on a video tape by means of the S-VHS VCR (Panasonic AG-7350). All measurements have been digitalized using the analog video capture card (Pinnacle DC10) and saved in non-compressed RGB format with a resolution of 720×580. An ensemble of 1400 images per measurement is used for the statistical analysis.

The calibration has been conducted in situ by heating water in the channel. The camera and light source have been in the same position during the measurements and calibration process. The temperature step during calibration is 0.2 °C and 400 images are captured per calibration step. The Hue value is calculated from the RGB space using formula

$$\mathrm{Hue} = \begin{cases} \arccos\left\{\frac{\frac{1}{2}[(\mathrm{R}-\mathrm{G})+(\mathrm{R}-\mathrm{B})]}{\sqrt{(\mathrm{R}-\mathrm{G})^2+(\mathrm{R}-\mathrm{B})(\mathrm{G}-\mathrm{B})}}\right\}; & \mathrm{G}-\mathrm{B} \geqslant 0 \\ 2\pi - \arccos\left\{\frac{\frac{1}{2}[(\mathrm{R}-\mathrm{G})+(\mathrm{R}-\mathrm{B})]}{\sqrt{(\mathrm{R}-\mathrm{G})^2+(\mathrm{R}-\mathrm{B})(\mathrm{G}-\mathrm{B})}}\right\}; & \mathrm{G}-\mathrm{B} < 0 \end{cases}$$

Here R, G and B are normalized with a maximal value of red, green and blue color (for 8 bit precision, which is valid in this research, the maximal value is 255). The temperature is calibrated versus Hue-value. Because of the steep gradient in the region of the blue color the calibration curve is divided in two parts: from the beginning of the red color (20 °C in our case) till the first part of the blue range (23 °C). The first part of the curve is fitted with the third order polynomial. The remaining part of the blue range is fitted by means of the fifth order polynomial. In this way a wiggle, which would been produced at the ends of calibration curves, if the eight order polynomial fitting had been applied on the full band at once, is avoided and the fitting error is reduced to minimum. Because of the non-homogeneous TLCs and their surface illumination, an image is divided into small interrogation areas of the size 2×2 pixels. For each interrogation area the calibration curves are calculated. The calibration accuracy is within 0.1° in the red–green zone and within 0.3° in the blue zone.

Since the plexiglas surface can be treated as an adiabatic wall, the effectiveness is calculated from the temperature measurements as

$$\eta = \frac{T_{\mathrm{wall}} - T_\infty}{T_{\mathrm{jet}} - T_\infty}$$

Here T_∞ is the temperature of the cross-flow, T_{jet} is the jet temperature and the temperature measured on the plate wall is denoted as T_{wall}. From this the uncertainty of the adiabatic film cooling effectiveness can be calculated as

$$\Delta\eta^2 = \left(\frac{\partial\eta}{\partial T_{\mathrm{wall}}}\Delta T_{\mathrm{wall}}\right)^2 + \left(\frac{\partial\eta}{\partial T_{\mathrm{jet}}}\Delta T_{\mathrm{jet}}\right)^2 + \left(\frac{\partial\eta}{\partial T_\infty}\Delta T_\infty\right)^2$$

Temperature of the jet and cross-flow have been measured with the same thermometer. Therefore, the uncertainty $\Delta T_{\mathrm{jet}} = \Delta T_\infty = 0.05$ °C. If the uncertainty of the wall temperature is written as $\Delta T_{\mathrm{wall}} = n\Delta T_{\mathrm{jet}}$, we obtain the following equation for the adiabatic film cooling effectiveness:

$$\Delta\eta = \frac{\Delta T_\infty}{T_{\mathrm{jet}} - T_\infty}\sqrt{n^2 + \eta^2 + (\eta - 1)^2}$$

$\Delta\eta$ has maximum values for $\eta = 0$ or $\eta = 1$ which gives

$$\Delta\eta_{\max} = \frac{\Delta T_\infty}{T_{\mathrm{jet}} - T_\infty}\sqrt{1 + n^2}$$

The uncertainty of the effectiveness measured in this way depends on n which represents the quality of the calibration. For $n = 1$, $\Delta\eta = 0.012$ and for $n = 6$, $\Delta\eta$ is 0.051. n is around 2 in the gradual part of the calibration curve and reaches 6 for the steep side. Therefore, the absolute effectiveness error is 0.02 for $0 < \eta < 0.65$ and $\Delta\eta = 0.05$ if $\eta > 0.65$.

The volume flow is measured with a flow meter located in front of the plenum with an error of 2% and the channel velocity is measured by means of particle image velocimetry. The Reynolds number, based on the cross-flow velocity and location of the hole is constant for all measurements and it is $Re_l = \frac{V_\infty l}{\nu} = 3.23 \times 10^5$. The velocity ratio is varied from 0.15 to 1.5 by means of changing the jet volume flow. Hence, the jet Reynolds number (based on the averaged jet velocity and diameter of the hole D) is between $Re_l = \frac{\overline{V}_{\mathrm{jet}} D}{\nu} = 1.70 \times 10^3$ and 1.70×10^4. Furthermore, the Richardson number, defined here as $Ri = \frac{g\beta D\Delta T}{V_\infty^2}$, is 0.015 which means that the buoyancy forces can be neglected and the heat transfer is dominated by forced convection. In the equations ν is the kinematic viscosity, l is the distance of the leading edge of the hole from the plate leading edge, g is the acceleration in the gravitational field, ΔT is the difference between the jet and cross-flow temperature and β is the thermal expansion coefficient. The Richardson number based on the jet velocity is proportional to the

above defined Richardson number. The proportionality factor is $1/\mathrm{VR}^2$, which gives the highest Richardson number of 0.25 for $\mathrm{VR} = 0.25$. This means that the buoyancy forces could influence the secondary flow structures inside the jet at low velocity ratios.The effect of the horizontal conduction in the measuring plate on the sharpness of the measured temperature gradients can be estimated from the following. The heat input from the fluid to the plate in a Blasius flow would be:

$$q(x) = 0.332\frac{k}{x}Re_x^{1/2}Pr^{1/3}\Delta T$$

which in our measurements at the position of the nozzle gives $q \approx 110\Delta T\ \mathrm{W/m^2}$. If this input heat-flux is equated to an (imaginary) horizontal heat-flux over the same temperature difference:

$$q_\mathrm{h} = \frac{k_\mathrm{plate}\Delta T}{\ell}$$

the length scale ℓ can be solved. This gives $\ell \approx 2$ mm. This means that horizontal conduction within the plate will smooth gradients with a length scale smaller than ℓ ($\approx 0.04D$).

3. Results and discussion

3.1. Two-dimensional plots

In this section the film cooling effectiveness is presented as two-dimensional contour plots. The minimal visualized effectiveness is bounded with a contour line of 0.1 and the increment is also 0.1. The influence of the imperfection and its position on the adiabatic film cooling effectiveness are presented and analyzed at four different velocity ratios ($\mathrm{VR} = 0.25;\ 0.50;\ 1.0;\ 1.5$).

Fig. 3 depicts the effectiveness at $\mathrm{VR} = 0.25$. The effectiveness at the low velocity ratio is qualitatively the same for the perfect hole and for the hole with an imperfection. The effectiveness larger than 0.1 spreads in lateral direction from -0.75 to 0.75 which gives a coverage of $1.5D$. In the streamwise direction cooling is well established till the end of the measurement field, with $\eta = 0.2$ at $x = 8.5D$ from the hole trailing edge. The higher contour lines have a triangular shape which covers almost the same area independently of the imperfection. The maximal measured effectiveness is slightly larger than 0.7. This large effectiveness is absent only in the case in which the half-torus is placed at the exit of the hole. The cooling surface is fairly symmetric. A reason for a small skew of the cooled surface is probably due to a small compound angle of the hole, which is around 2°.

At the low velocity ratios ($\mathrm{VR} \approx 0.25$–0.4) the jet may be expected to bent strongly at the windward side and attach immediately to the wall. This leads to a maximal effectiveness detected in the near vicinity of the hole (1.7–$2.5D$). Subsequent mixing in the near region (2.5–$6D$) decreases the effectiveness by about 50%. When the velocity ratio is increased to 0.50 (Fig. 4) the influence of the imperfection

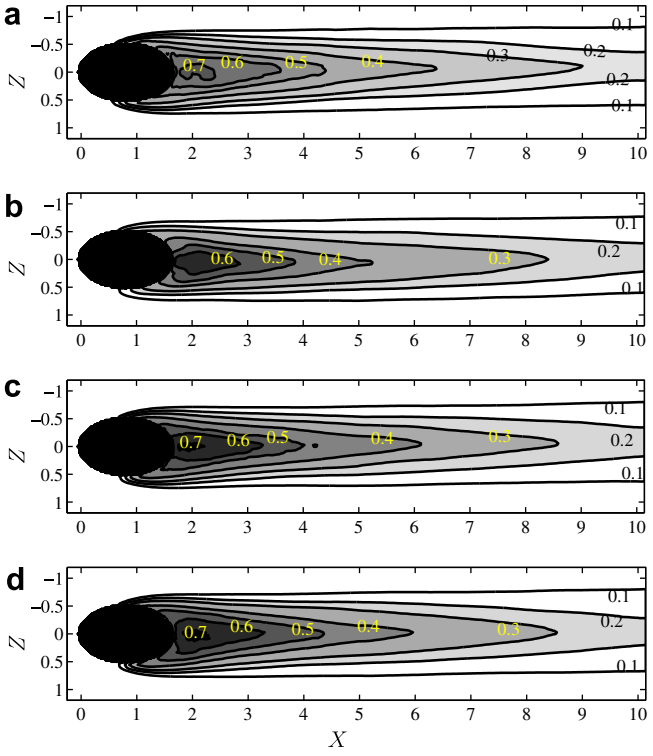

Fig. 3. Film cooling effectiveness at the velocity ratio 0.25 in the: (a) perfect, (b) IT1, (c) IT2 and (d) IT3 case.

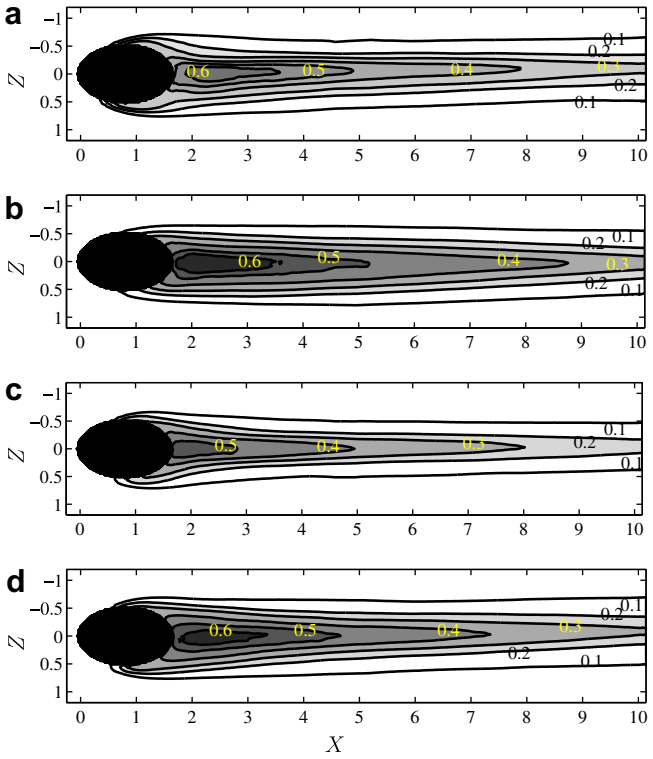

Fig. 4. Film cooling effectiveness at the velocity ratio 0.50 in the: (a) perfect, (b) IT1, (c) IT2 and (d) IT3 case.

becomes visible. In the perfect case the cooled surface ($\eta \geqslant 0.1$) is elongated. At the end of the measurement field

an effectiveness of 0.3 is detected but the lateral coverage is slightly smaller than at VR = 0.25. The highest detected effectiveness is 0.6. It is detected in the vicinity of the hole but not on the hole trailing edge. The imperfection deep inside the hole, i.e. inner-torus 3, does not have a strong influence at this velocity ratio. The half torus on the second position (inner-torus 2) deteriorates the effectiveness and narrows the cooled surface. The maximal effectiveness of about 0.5 is detected on the trailing edge and the vicinity of the hole. At the end of the measurement field the lateral coverage drops below 1D and slightly exceeds 0.2. When the half-torus is placed at the exit of the hole (inner-torus 1) the film cooling effectiveness is qualitatively similar to the perfect case but it is better distributed and more spread in the lateral direction.

A further increase of the velocity ratio to 1.00 (see Fig. 5) decreases the film cooling effectiveness. If the jet is ejected through the perfect hole the effectiveness is around 0.1 in the vicinity of the hole trailing edge. In the near field it reaches 0.4 and decreases continuously to 0.2 at the end of the measurement field. The lateral coverage of $\eta = 0.1$ is less than 1D in the perfect case. The half-torus on the third position ensures the better effectiveness in the vicinity of the hole. In the near field and in the intermediate region, the effectiveness decreases below the effectiveness in the perfect case. The maximal effectiveness is 0.3 and the lateral coverage around 0.5D. The inner-torus 2 ensures the maximal effectiveness at the trailing edge of the hole and decreases continuously downstream. The cooled surface is smaller than in the inner-torus 3 and perfect case. The inner-torus 1 enhances both the film cooling effectiveness and the surface coverage. The maximal η is larger than 0.5 and the maximal width is equal to 2D. The effectiveness of 0.3 is still detected at the end of the measurement field which is 50% higher than in the perfect case.

At VR = 1.5 (see Fig. 6) cooling is absent in the vicinity of the hole in the perfect case. The contour of $\eta = 0.1$ appears at $x = 3.1D$ and extends till the end with a width of 0.5D. The inner-torus 3 increases cooling in the vicinity of the hole and has a similar effect in the near and intermediate field. The inner-torus 2 forms a bit wider but also shorter cooled surface than the perfect hole with rather similar values. The inner-torus 1 ensures good film cooling. With the maximal effectiveness of 0.3 and the width of 1.5D ($\eta \approx 0.2$ at the end of the measurement field).

The best cooled surface is found for VR = 0.70 in the case of the inner-torus 1. The lowest is found at VR = 1.5 in the perfect, inner-torus 2 and inner-torus 3 cases. It is worthwhile to notice that conductive effects in the plate material will have a slight spreading effect on the measured effectiveness. This means that the effect of the changes that cause the optimal performance of IT1 are underestimated: conduction in the plate slightly masks the decrease of the effectiveness in the vicinity of the perfect hole and spreads the high effectiveness of the IT1 on the centerline.

In Fig. 7a central line effectiveness ($z = 0$) for the perfect hole is compared to other experimental results available

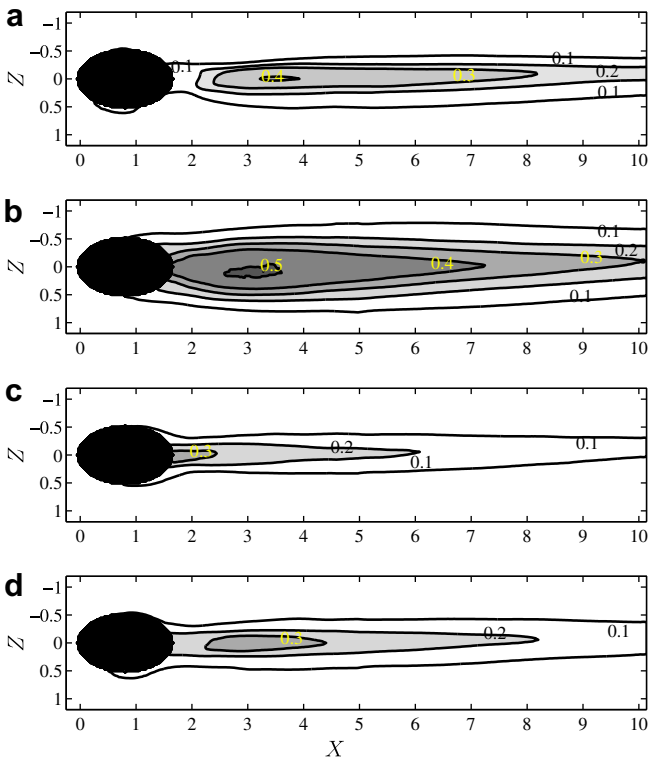

Fig. 5. Film cooling effectiveness at the velocity ratio 1.00 in the: (a) perfect, (b) IT1, (c) IT2 and (d) IT3 case.

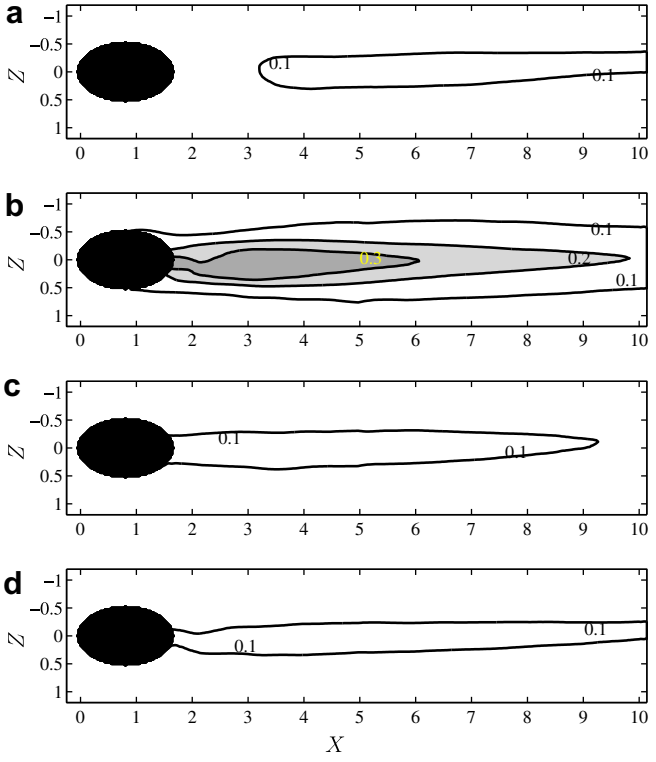

Fig. 6. Film cooling effectiveness at the velocity ratio 1.50 in the: (a) perfect, (b) IT1, (c) IT2 and (d) IT3 case.

from the literature. It should be noted that the experimental results are obtained with injection holes at slightly different

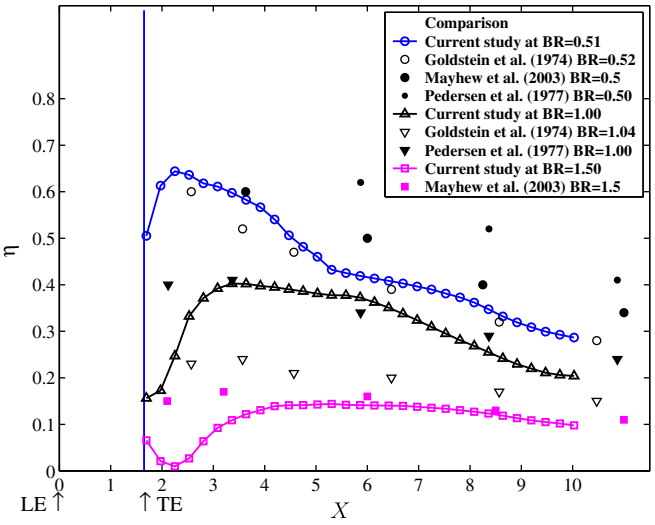

Fig. 7. Central line effectiveness compared with the data from the literature.

angles. At VR = 0.50 results are in agreement with the Goldstein and Eckert (1974) and Mayhew et al. (2003) but undershoots the values from Pedersen et al. (1977). At VR = 1.0 the effectiveness agrees with Pedersen et al. (1977) but overshoots the measurements of Goldstein and Eckert (1974). In the near and intermediate field results agree with Mayhew et al. (2003) at VR = 1.5. These differences can probably be attributed to the state and the size of the approaching boundary layer of the cross-flow and the momentum ratio which are not the same in compared cases.

In Jovanović (2007) an experimental study of the interaction of the flow field and the film cooling effectiveness is presented. Two major effects are distinguished:

- Imperfections lead to a larger momentum ratio and an additional vortex at the windward side which can lead to a burst of the jet and strong mixing with the cross-flow (see Fig. 8). This mechanism is responsible for the decreased effectiveness for IT2.
- The imperfection at the exit of the hole ensures better and wider coverage, which can be attributed to its influence of the generated counter rotating (side-) vortices (see Fig. 9). Their decreased intensity leads to a decreased suction of main stream fluid into the jet flow and, therefore, strongly increases the effectiveness in the near-wake.

3.2. Integral curves

Although two-dimensional plots contain detailed information about the film cooling effectiveness it is difficult to extract representative quantitative information for a large number of measurements. To summarize the effect of the velocity ratio simultaneously with the effect of the imperfection position and the influence of the free stream turbulence intensity the equivalent cooled surface is defined as:

$$\phi = \frac{1}{\Delta T_{j\infty}} \int_{X_{\text{trailing edge}}}^{+\infty} \int_{-\infty}^{+\infty} (\Delta T_{j\infty} - \Delta T_{j\text{fw}})\, \mathrm{d}z\, \mathrm{d}x$$

where $\Delta T_{j\infty} = T_\infty - T_{\text{jet}}$, $\Delta T_{j\text{fw}} = T_{\text{film at wall}} - T_{\text{jet}}$. If T_∞ and T_{jet} are constant ϕ can be calculated as:

$$\phi = \int_{x_{\text{trailing edge}}}^{+\infty} \int_{-\infty}^{+\infty} \eta\, \mathrm{d}z\, \mathrm{d}x$$

The equivalent cooled surface is the area over which the effectiveness is equal to 1 and its size is equal to the double integral of the film cooling effectiveness. Here the equivalent cooled surface is normalized and calculated as:

$$\Phi = \frac{\phi}{D^2} = \frac{\Delta x \Delta z}{D^2} \sum_{i=1}^{M} \sum_{j=1}^{N} \eta_{i,j}$$

where Δx and Δz are the discrete steps between two calculated $\eta_{i,j}$ points and it is constant for all of them. $i = 1$ is positioned at the trailing edge of the hole and $i = M$ is located 8 diameters downstream from the hole trailing edge, while $j = 1$ and $j = N$ correspond to the positions $-1.5D$

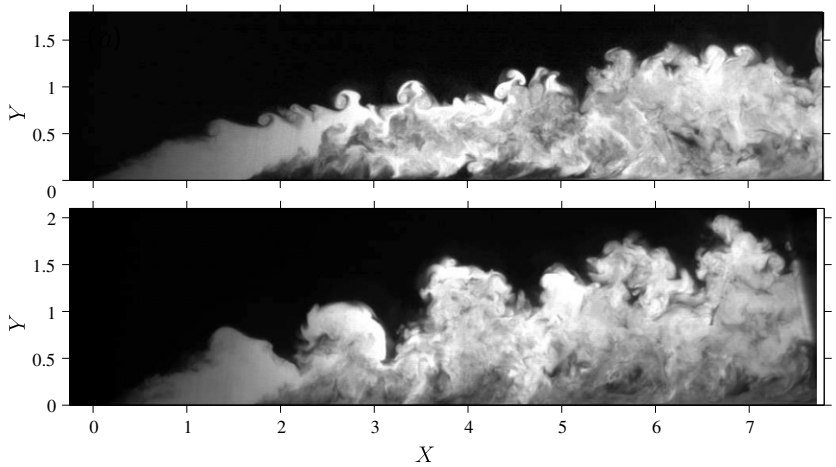

Fig. 8. LIF-coloring of the jet at VR = 1 for the (a) perfect hole and (b) IT2.

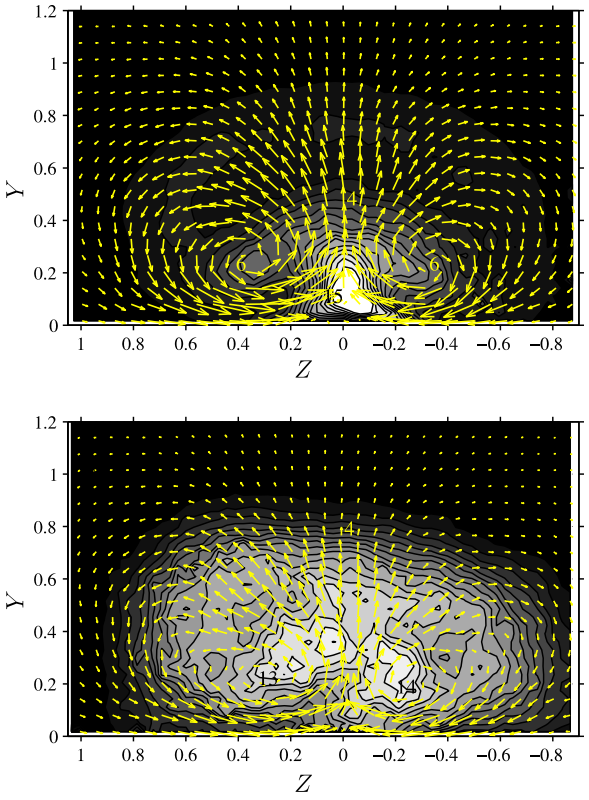

Fig. 9. The tail view of the vortical structures at VR = 1 (the gray-scale represents the turbulence level) for the (a) perfect hole and (b) IT1.

and+1.5 from the hole side edges. Using the equivalent cooled surface to compare the different geometries removes the issue of horizontal conduction in the plate.

The normalized equivalent cooled surface (Φ) is depicted in Fig. 10 for the five different geometries at varying velocity ratios from 0.15 to 1.5. In Fig. 10a the flow conditions are the same as for the experiments described in the previous paragraph. At VR = 0.15, Φ in the perfect case is 3.2 and all other data scatter within the measurement error. Φ increases and reaches its maximum of 3.6 for VR = 0.25 in the perfect case. At this low velocity ratio, the imperfection has very little influence on the equivalent cooled surface. The imperfection influence starts to be visible at about VR = 0.5. The inner-torus 1 improves Φ by about 20% while the inner-torus 2 deteriorates it by 30%. The influence of the triple imperfection is also negative, which indicates the dominance of the negative effect of the inner-torus 2. The inner-torus 3 does not show any significant effect. At a velocity ratio VR ≈ 0.7, Φ is about 2.1 in the perfect case. The inner-torus 1 creates the largest Φ of 4.1. This is almost 100% larger than in the perfect case. The inner-torus 2 still reduces Φ by about 30%. The equivalent cooled surface produced by means of the triple imperfection is almost a linear combination of the effectiveness produced by the inner-torus 1 and 2. At VR = 1.0, Φ drops to 1.7 for the perfect case but relatively to the other cases it does not change. At this VR a small influence of the inner-torus 3 is detected. Although this change is a bit larger than the measurement error it can be concluded that the film cooling effectiveness is rather sensitive around VR = 1.0. The benefit of inner-torus 1 rises with increasing VR while the negative effect of inner-torus 2 decreases. At the last measured VR = 1.5, Φ in the perfect case is equal to 0.7. The negative influence of the inner-torus 2 has vanished. Instead, it increases Φ by 20%. The increase of the effectiveness for of the inner-torus 1 at VR ≈ 1.5 is about a factor 2.5.

The important parameter which could not be neglected is the free steam turbulence level. To obtain a higher turbulence intensity a static grid is placed at the entrance of the test section. The effect of the turbulence intensity on the equivalent cooled surface is depicted in Fig. 10. The position of the imperfection is varied. The full symbols represent the data measured at the low free stream turbulence level and are shown in Fig. 10a. The data represented with open symbols capture the behavior of Φ at the higher turbulent level (see Fig. 10b). Turbulence does not show any

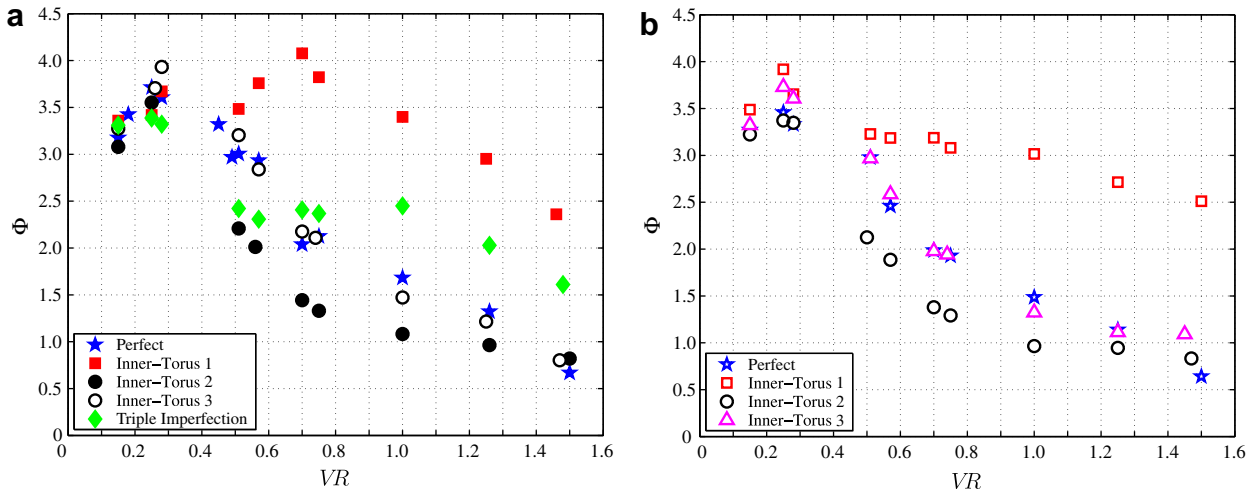

Fig. 10. The equivalent cooled surface at: (a) low free stream turbulence intensity ($Tu \approx 1\%$) and (b) larger free stream turbulence intensity ($Tu \approx 7\%$).

significant influence on the perfect, inner-torus 2 and inner-torus 3 cases. However, for $0.5 < VR < 1$, *Tu* influences the effectiveness for inner-torus 1. *Tu* decreases all values of Φ for this case and the highest difference is measured at $VR \approx 0.7$. If $VR > 1$ the influence of the free stream turbulence intensity becomes much smaller and it is almost negligible.

A few vortical structures have been detected in the jet cross-flow interaction with a film cooling characteristic. These structures affect the film cooling process (see Jovanović et al., 2005). The largest are the lee, windward vortices and a counter rotating pair known also as kidney vortices. The kidney vortices are the most responsible for the heat and momentum transfer. At small velocity ratios the kidney vortices are small and dissipate very fast. The turbulent mixing becomes dominant near the hole. Therefore, the effectiveness is similar for all investigated cases. At $VR = 0.50$ the kidney vortices are detectable in the perfect case. They enhance the heat transfer and reduce the effectiveness. In the inner-torus 2 case the lee and windward vortices are amplified. These vortices generate the bursting mechanism and the jet collapses. This collapse directs the flow of the free stream towards the plate wall and decreases the film cooling effectiveness more than the kidney vortices in the perfect case. The additional separation ensured with the inner-torus 1 and 2, improves the effectiveness in the immediate vicinity of the hole at larger velocity ratios. The inner-torus 1 forms a quasi-expanded hole. The kidney vortices are small and dissipate very fast and probably the bursting mechanism does not occur. This ensures a better coverage and the larger effectiveness than in the perfect case.

4. Conclusion

In this paper the influence of the discrete imperfection inside the cylindrical inclined hole on the adiabatic film cooling effectiveness is studied. The film cooling is simulated with the jet cross-flow interaction. The half torus is used to imitate the real imperfection. Wall temperature is measured by means of liquid crystal thermography. Last measured point is located 8.5*D* downstream from the hole leading edge. The velocity ratio, position of the imperfection, number of imperfections and turbulent intensity are varied and their influence on the film cooling effectiveness is analyzed.

The velocity ratio has a large influence on the film cooling effectiveness. It is concluded that in the perfect case and with the inner-torus 2 and 3 the best effectiveness is achieved at low velocity ratios of about 0.4. The inner-torus 1 generates the largest effectiveness at $VR \approx 0.7$.

The imperfection on the first position, in the immediate vicinity of the hole exit, has a very small influence on the effectiveness at small velocity ratios. Starting from $VR = 0.5$ the inner-torus 1 has a positive effect which rises with a further increase of the velocity ratio. Although, the absolute effectiveness decreases with the velocity ratio, it is less sensitive than in the perfect case. At $VR \approx 1.5$ the benefit of the inner-torus 1 is leads to an effectiveness increase of about a factor 2.5.

The imperfection located 1.2 diameter inside the hole (called here as inner-torus 2) at the low velocity ratios does not have any influence on the film cooling effectiveness. At the moderate velocity ratios (around $VR = 0.5$) the inner-torus 2 decreases significantly the effectiveness and narrows the cooled area. At larger velocity ratios ($VR = 1.5$) an influence of the inner-torus 2 almost vanishes.

The imperfection located 2.5 diameters inside the hole (called here as inner-torus 3) does not have any significant influence on the film cooling effectiveness.

If three similar imperfections are simultaneously placed at all three positions the negative influence of the inner-torus 2 prevails if $0.5 < VR < 0.6$. If $VR > 0.6$ the influence of the triple imperfection can be approximated as a linear combination of the inner-torus 1 and 2.

The free stream turbulence is changed by means of using static grid. The turbulence intensity is increased from 1% to 7%. The adiabatic effectiveness is weakly affected by the turbulent intensity. Only in the vicinity of the maximum effectiveness for the inner-torus 1 (around $VR = 0.7$), the effectiveness is reduced for about 10%. In all other cases the effect of turbulence intensity can be neglected.

References

Allmen, M. van, Blatter, A., 1995. Laser-beam Interaction with Metal. Springer-Verlag, pp. 115–134.

Bergeles, G., Gosman, A.D., Launder, B.E., 1976. The near-field character of a jet discharged normal to a main stream. ASME J. Heat Transfer, 373–379.

Cho, H.H., Kim, B.G., Rhee, D.H., 1998. Effects of hole geometry on heat (mass) transfer and film cooling effectiveness. In: Proceedings of 11th IHTC, Vol. 6, Kyongju, Korea.

Goldstein, R.J., Eckert, E.R.G., 1974. Effects of hole geometry and density on three-dimensional film cooling. Int. J. Heat Mass Transfer 17, 595–607.

Guo, X., Schröder, W., Meinke, M., 2006. Large-eddy simulation of film cooling flows. Comp. Fluids 35, 587–606.

Hale, C.A., Plesniak, M.W., Ramadhyani, S., 2000. Film cooling effectiveness for short film cooling holes fed by a narrow plenum. ASME J. Turbomach. 122, 553–557.

Haven, B.A., Kurosaka, M., 1997. Kidney and anti-kidney vortices in crossflow jets. J. Fluid Mech. 352, 27–64.

Jovanović, M.B., de Lange, H.C., van Steenhoven, A.A., 2005. Influence of laser drilling imperfection on film cooling performances. ASME paper GT2005-68251, Reno-Tahoe, USA.

Jovanović, M.B., Lange, H.C. de, Steenhoven, A.A. van, 2006. Influence of hole imperfection on jet cross flow interaction. Int. J. Heat Fluid Flow 27, 42–53.

Jovanović, M.B., 2007. Film cooling through imperfect holes. PhD thesis, Eindhoven University of Technology, the Netherlands.

Lutum, E., Johnson, B.V., 1998. Influence of the hole length-to-diameter ratio on film cooling with cylindrical holes. ASME, paper 98-GT-10, Stockholm, Sweden.

Mayhew, J.E., Baughn, J.W., Byerley, A.R., 2003. The effect of freestream turbulence on film cooling adiabatic effectiveness. Int. J. Heat Fluid Flow 24, 669–679.

Lim, T.T., New, T.H., Luo, S.C., 2001. On the development of large-scale structures of a jet normal to a cross flow. Phys. Fluids 13, 770–775.

New, T.H., Lim, T.T., Luo, S.C., 2003. Elliptic jets in cross-flow. J. Fluid Mech. 494, 119–140.

Pedersen, D.R., Eckert, E.R.G., Goldstein, R.J., 1977. Film cooling with large density difference between the mainstream and the secondary fluid measured by the heat-mass transfer analogy. ASME J. Heat Transfer 99, 620–627.

Peterson, S.D., Plesniak, M.W., 2004. Evolution of jets emanating from short holes into crossflow. J. Fluid Mech 503, 57–91.

Rutledge, J.L., Robertson, D., Bogard, D.G., 2005. Degradation of film cooling performance on a turbine vane suction side due to surface roughness. ASME paper GT2005-69045, Reno-Tahoe, USA.

Yuen, C.H.N., Martinez-Botas, R.F., 2003. Film cooling characteristics of a single round hole at various streamwise angles in a crossflow: Part I effectiveness. Int. J. Heat Mass Transfer 46, 221–235.